RTM amplitude correction in angle-domain based on Poynting vectors

*Liu Ji-cheng**[1,2] Xie Xiao-bi[2] Chen bo[3]*

1 School of Electric and Automatic Engineering, Changshu Institute of Technology,Changshu, P. R. China, 2 Institute of Geophysics and Planetary Physics,University of California at Santa Cruz, CA,U.S.A., 3 School of Earth Science and Geological Engineering,SUN YAT-SEN University, Guangzhou,, P. R. China

Summary

Image correction in angle-domain based on Poynting vector is recommended. By using Poynting vector to decompose wavefields and construct local illumination matrix, We compute full-wave-equation-based illumination in time domain and acquisition aperture response. After the regular RTM image is decomposed into common dip images, an effective amplitude correction method in dip angle domain is deduced. Numerical example for SEG model is conducted to demonstrate the applications of this method

Introduction

By researching the interaction of incident wave and reflected wave with reflector in angle domain, seismic illumination analysis (Wu et al., 2003; Xie et al., 2006; Xie et al., 2013), imaging resolution analysis, imaging correction(Xie et al., 2005; Wu et al., 2006, Yan et al., 2014), imaging gather extraction（Sava and Vasconcelos, 2011; Yan and Xie, 2012; Wang et al., 2013) ,and AVA analysis (Yan and Xie, 2012) can all be handled. Yoon et al. (2004) used Poynting vector to compute wavefields propagation direction and constructed angle domain imaging condition by introducing an angle-related filter to weight the different direction waves from sources and receivers, which restrained low wavenumber artifacts effectively. The purpose of migration is not limited to reveal the subsurface geometry, it is also dedicated to obtain the physical parameters of subsurface medium. But the limited acquisition aperture combined with complex velocity structure and reflector dip angle lead to irregular illumination to the subsurface regions. Seismic targeted-illumination analysis provides an effective quantitative tool for the influenced factors mentioned above and can be used to compensate image. In this paper, we decompose the wavefileds propagation angle by Poynting vectors and construct local ilumination matrix(LIM) in which the acquisition dip response(ADR) is calculated. The regular RTM image is decomposed by slant stacking to common dip angle images(CDI). Then an efficient amplitude correction method in dip-angle domain is proposed. Finally, we use 2D SEG model to demonstrate the results of amplitude correction.

Angle decomposition for migrated wavefields

Even there are some intrinsic problems such as stability and reliability to use Poynting vector to calculate the wave propagation direction, the method is still an efficient way to obtain high resolution angle information. A 2D Poynting vector can be express as(Yoon et al.,2011)

$$\boldsymbol{P} = (p_x, p_z) = -\nabla \boldsymbol{u} \cdot \frac{\partial \boldsymbol{u}}{\partial t} \tag{1}$$

Where $\boldsymbol{u}$ is either the source wavefield $\boldsymbol{u}_s$ or the receiver wavefield $\boldsymbol{u}_g$, t is time, x and z are the horizontal and the vertical coordinates respectively, $\nabla \boldsymbol{u}$ is spatial gradient, p_x and p_z is the horizontal and vertical components of Poynting vectors respectively. Then the wave propagation direction is

$$\theta = \arctan(\frac{p_x}{p_z}) \tag{2}$$

$\partial \boldsymbol{u}/\partial t$ and $\nabla \boldsymbol{u}$ can be easily acquired in staggered FD scheme without extra computation. Yoon et al. (2011) calculated Poynting vectors by Gaussian-weighted function in time domain. Thomas et al.(2011) used smoothing filter to Poynting vectors both in spatial and time domain. We use SEG model to compare the wave propagation directions calculated by slowness analysis and Poynting vectors respectively. The velocity model is overlapped by snapshot of wavefields in Figure1a, the shot locates at asterisk position. The orientation of these energy peaks in the polar coordinates gives propagation directions which are calculated by slowness analysis method, and the red arrows indicate propagation directions calculated by Poynting vectors. If only one wavefront is presented, the estimated directions by both methods are almost the same(Figure 1b-d). When there are more than one wavefront existing simultaneously, slowness analysis can give directions of individual wavefront, but Poynting vector method calculates the vectors sum of different wavefronts, which can only make a single estimation of propagation angle(Figure1e). Poynting vector method assumes only one direction at one grid point at each time step. Although Poynting vectors cannot separate wave propagation directions with multiple wavefronts overlapped, it observably decreases the computation of angle decomposition, which makes it have huge application potential. Still taking SEG model (Figure 1a) as an example, on the same computation condition, we calculate wave

2017 CGS/SEG International Geophysical Conference
Qingdao, China, 17-20 April 2017
*The corresponding author: ljcdqpi@163.com.

propagation angle of single shot by using slowness analysis and Poynting vectors respectively to compare computation time consumed. The time using slowness analysis is 16269.09s, but only 238.091s for Poynting vectors. The computation efficiency enhances about 68 times.

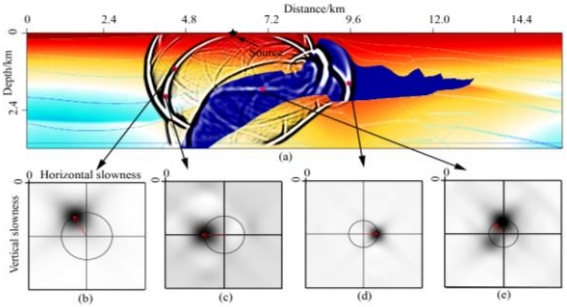

Figure 1. The snapshot of wavefields with velocity model overlapped (a),and wave propagation direction calculated by local plane wave decomposition method and Poynting vectors(b)-(e).(t=1.7 s)

RTM amplitude correction in angle-domain

Although low wavenumber artifacts can be suppressed to some extent with angle-domain filtering (Wang et al., 2013), there are still many factors, such as acquisition aperture, complex overburden structures and reflector dip angle, to make irregular illumination to subsurface regions, which leads to biased image amplitude. The seismic illumination analysis is an efficient tool to optimize the acquisition system design, evaluate the image quality and make corrections to image, resulting in more accurate subsurface physical parameter retrieval. Given the observation system, the illumination in time domain from shot $\boldsymbol{r}_s$ tosubsurface target $\boldsymbol{r}$ along θ_s direction is expressed as(Yang et al.,2008)

$$\boldsymbol{D}_s(\theta_s,\boldsymbol{r};\boldsymbol{r}_s)=\int\left|\boldsymbol{u}_s(t,\theta_s,\boldsymbol{r};\boldsymbol{r}_s)\right|^2\mathrm{d}t \tag{3}$$

In a similar way, the illumination in time domain from receiver $\boldsymbol{r}_g$ to target $\boldsymbol{r}$ along θ_g direction is also expressed as

$$\boldsymbol{D}_g(\theta_g,\boldsymbol{r};\boldsymbol{r}_g)=\int\left|\boldsymbol{u}_g(t,\theta_g,\boldsymbol{r};\boldsymbol{r}_g)\right|^2\mathrm{d}t \tag{4}$$

From eqations(3) and(4), the LIM of target location $\boldsymbol{r}$ in time domain can be expressed as

$$\begin{aligned}\boldsymbol{A}(\theta_s,\theta_g,\boldsymbol{r};\boldsymbol{r}_s,\boldsymbol{r}_g)&=\boldsymbol{D}_s(\theta_s,\boldsymbol{r};\boldsymbol{r}_s)\cdot\boldsymbol{D}_g(\theta_g,\boldsymbol{r};\boldsymbol{r}_g)\\&=\int[\boldsymbol{u}_s(t,\theta_s,\boldsymbol{r};\boldsymbol{r}_s)]^2\mathrm{d}t\cdot\int[\boldsymbol{u}_g(t,\theta_g,\boldsymbol{r};\boldsymbol{r}_g)]^2\mathrm{d}t\end{aligned} \tag{5}$$

Where θ_s and θ_g are calculated by using equation (2). If the observation system is composed of multiple shots and geophones, the LIM from the whole acquisition system can be obtained by summing up contributions from individual source and receiver pairs

$$\boldsymbol{A}(\theta_s,\theta_g,\boldsymbol{r})=\sum_{\boldsymbol{r}_s}\sum_{\boldsymbol{r}_g}\boldsymbol{A}(\theta_s,\theta_g,\boldsymbol{r};\boldsymbol{r}_s,\boldsymbol{r}_g) \tag{6}$$

Shown in Figure 2 displays the LIMs of six points in SEG model. The observation includes 350 shots with an interval of 48.77 m, each shot is matched with 176 left-side receivers separated by 24.38m. The shot records are modeled with the 4th order accuracy in space and 2nd order in time finite-difference method with a 15 Hz Ricker wavelet and PML absorbing boundary. The illumination scope mainly concentrates left-upper corner in every LIM because of using single-side receivers. The region windowed by the white square is the range of incident and scattering angle limited within $\pm90^0$,which is the illumination scope for one-way propagator. For full-wave method, the illumination approaches $\pm180^0$ for both incident and scattering wave. It can be seen from the figure that the illumination apertures are wide at shallow regions, but the apertures become narrower with increasing depth. Because of shadowing effect, the illumination at subsalt region is distinctly weak, which influences the final imaging quality.

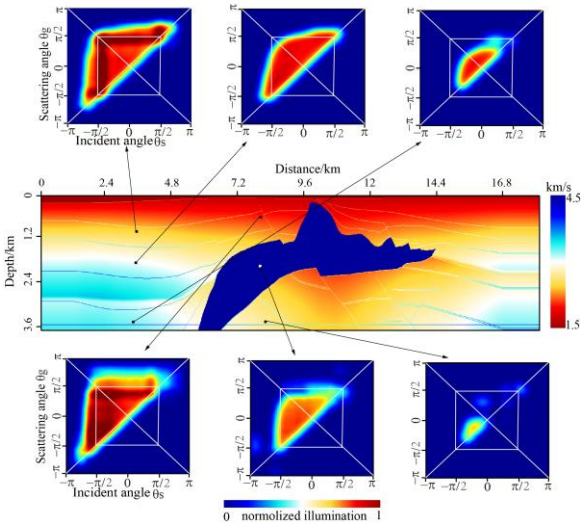

Figure 2 Local image matrix of different locations in SEG model

ADR is the total illumination for a target with a specified dipping angle when given the observation system,which can be obtained from the LIM by adding up $\boldsymbol{A}(\theta_s,\theta_g,\boldsymbol{r})$ over θ_s and θ_g which makes θ_d equal to the given dipping angle. By decomposing the regular RTM image into CDIs and normalizing CDI with ADR, the image amplitude can be corrected with summation of all the normalized CDIs. On the basis of angle transform, (θ_s,θ_g) is transformed into (θ_r,θ_d), then ADR is expressed as

$$\boldsymbol{ADR}(\theta_d,\boldsymbol{r})=\int\boldsymbol{A}(\theta_r,\theta_d,\boldsymbol{r})\mathrm{d}\theta_r, \tag{7}$$

The image corrected by ADRs is

$$\boldsymbol{I}_{\mathrm{c}}(\boldsymbol{r})=\int\frac{\boldsymbol{I}(\theta_{\mathrm{d}},\boldsymbol{r})}{\boldsymbol{ADR}(\theta_{\mathrm{d}},\boldsymbol{r})}\mathrm{d}\theta_{\mathrm{d}}\quad,\qquad(8)$$

Where $\boldsymbol{I}(\theta_{\mathrm{d}},\boldsymbol{r})$ is CDI, $\boldsymbol{I}_{\mathrm{c}}(\boldsymbol{r})$ is the image corrected.

Numerical Example

Poynting vectors can be calculated directly during wave propagating, so we don't need to decompose Green's function when using Poynting vectors to calculate angles. But computing angles at each grid and each time will be very time-consuming and need very large memory. Hu et al. (2104) pointed out that it has higher reliability by using higher wave amplitude to estimate angle information. Yang et al.(2008) also gave the similar results. So for each grid point, the wave propagation angle can be calculated only at the times when a few the highest amplitude of the wavefield occurs. In addition, using slant stacking decomposes the full-stacked image into CDIs. Because ADR is the smooth function in space domain, it can be computed at a coarse grid and then interpolated into the image grid(Yan et al., 2014).

Adapting the same observation system as in Figure 2, the CDIs with the dip angles -15 °,15 °,-45 ° and 45 °, are shown in Figure 3. Figure 4 displays the corresponding ADRs. It can be seen that the amplitude of CDIs is coincident with the strength of ADRs. Figure 5 displays each CDI corrected by the corresponding ADR. Summing up all the corrected images forms the final image, as shown in Figure 6. The image amplitude of different reflectors become more balanced after correction, especially the subsalt regions with steep structures are enhanced and become more continuous. Figure 7 compares the theoretical normal reflectivity(red lines) and the image amplitudes. The image amplitudes are consistent basically with the theoretical value in shallow regions whatever corrected or not. But in deep areas, especially in the subsalt regions, the regular image amplitudes are very weak and have large difference compared with the theoretical reflectivity because of the irregular illumination, while the image amplitudes after corrected match with the theoretical values very well.

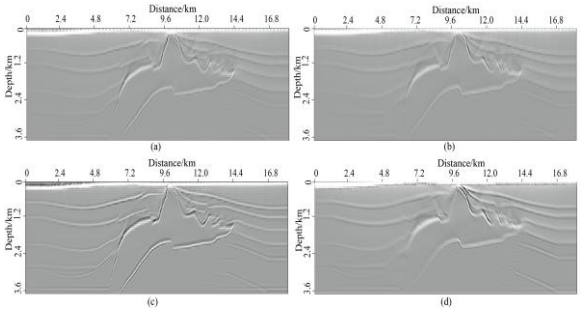

Figure 3 CDIs with dip angle: (a)-15 °,(b)15 °,(c) -45 °,(d) 45 °

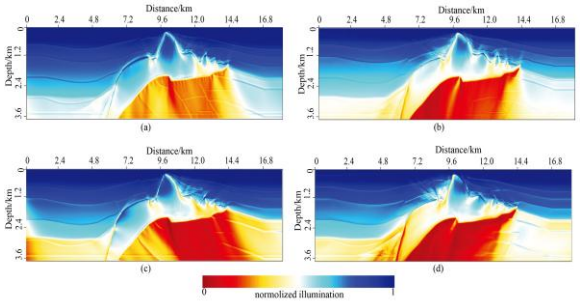

Figure 4 ADRs with dip angles: (a)-15 °,(b)15 °,(c) -45 °,(d) 45 °

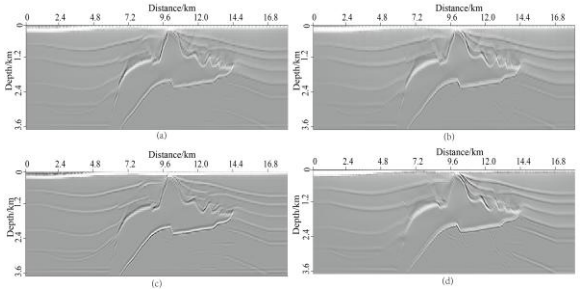

Figure 5 The corrected CDIs with dip angles: (a)-15 °,(b)15 °, (c) -45 °, (d) 45 °

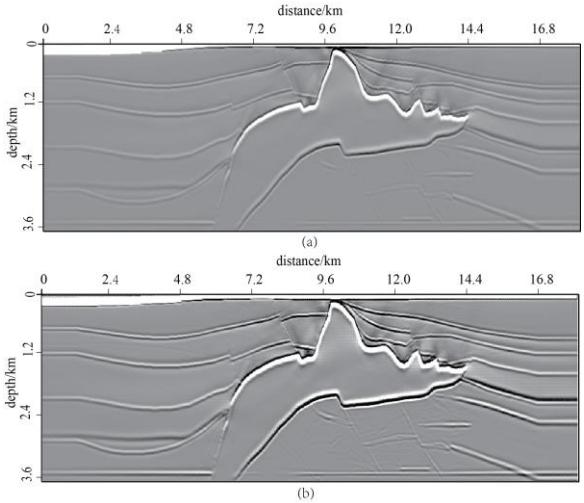

Figure 6 (a) the regular RTM image,(b) the image corrected by ADR

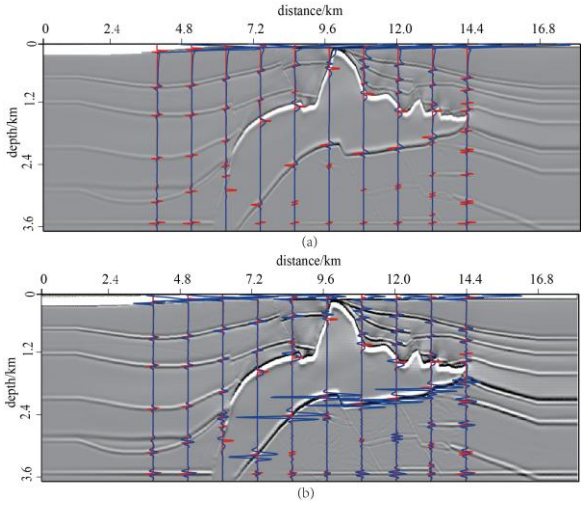

Figure 7 Theoretical reflectivity(red) versus image amplitudes(blue) (a)before compensation and (b)after compensation

Conclusions

A Poynting vectors based method for image amplitude correction in angle domain and is proposed in this paper. We calculate wave propagation directions based on Poynting vectors and construct local illumination matrix, which is used to calculate ADR. The regular RTM image is decomposed by slant stacking into CDIs which are compensated by the corresponding ADRs, then the final corrected image can be obtained by stacking all the compensated CDIs. The numerical tests demonstrate that the ADR correction improves image quality very well. Although there are inaccuracy and instability in angle estimation, Poynting Vector method can still achieve reasonable accurate result for complex models. Compared with local plane wave decomposition based on slant stacking or windowed FFT, the Poynting vectors method reduces computation time greatly.

REFERENCES:

Hu, Jin, G.A. McMechan and H. M. Guan, 2014, Comparison of methods for extracting ADCIGs from RTM. *Geophysics*, 79(3): 89–103.

Sava P, Vasconcelos I.,2011, Extended imaging conditions for wave equation migration. *Geophysical Prospecting*, 59(1): 35-55.

Thomas A D, Graham Q W.,2011, RTM angle gathers using Poynting vectors. 81th Annual Meeting, SEG Expanded Abstracts, 3 109-3113.

Wang Baoli, Gao Jinghuai, Chen Wenchao, et al., 2013, Extracting Efficiently Angle Gathers Using Poynting Vector During Reverse Time Migration. Chinese Journal of Geophysics, 56(1): 262-268.

Wu Rushan, Chen Ling and Xie Xiaobi, 2003, Directional illumination and acquisition dip-response. 65th Conference and Technical Exhibition, EAGE, Expanded abstracts, (Z-99): 1-4

Wu Rushan, Chen Ling, 2006, Directional illumination analysis using beamlet decomposition and propagation. *Geophysics*, 71(4): S147-S159.

Xie Xiaobi, Wu Rushan, Fehler M et al., 2005, Seismic resolution and illumination: A wave equation based analysis. 75th Annual International Meeting, SEG, Expanded Abstracts, Houston, 1862–1865.

Xie Xiaobi, Jin Shengwen, and Wu Rushan, 2006, Wave-equation based seismic illumination analysis. *Geophysics*, 71(5): S169–S177.

Xie Xiaobi,He Yongqing, Li Peiming, 2013,Seismic Illumination Analysis and Its Applications in Seismic Survey Design. Chinese Journal of Geophysics, 56(5): 1-14.

Yan Rui, Xie Xiaobi, 2012, An angle-domain imaging condition for elastic reverse time migration and its application to angle gather extraction. *Geophysics*, 77(5): 105–115.

Yan Rui. Guan Huimin, Xie Xiaobi, and Wu Rushan, 2014, Acquisition aperture correction in the angle domain toward true-reflection reverse time migration. Geophysics, 79, S241-S250.

Yang Hui, Xie Xiaobi, 2008,Target oriented full-wave equation based illumination analysis. 75th Annual International Meeting, SEG, Expanded Abstracts, 2216-2220.

Yoon K, Marfurt and Starr W., 2004, Challenges in reverse-time migration. 74th Annual International Meeting, SEG Expanded Abstracts, 1057–1060.

Yoon K, Guo M H, Cai J, et al., 2011,3D RTM angle gathers from source wave propagation direction and dip of reflector. 81th Annual International Meeting, SEG Expanded Abstracts, 3136-3140.